JACS
JOURNAL OF THE AMERICAN CHEMICAL SOCIETY

COMMUNICATION

pubs.acs.org/JACS

Spontaneous Formation of Wurzite-CdS/Zinc Blende-CdTe Heterodimers through a Partial Anion Exchange Reaction

Masaki Saruyama,[†] Yeong-Gi So,[‡] Koji Kimoto,[‡] Seiji Taguchi,[§] Yoshihiko Kanemitsu,[§] and Toshiharu Teranishi*[,†,§]

[†]Department of Chemistry, Graduate School of Pure and Applied Sciences, University of Tsukuba, 1-1-1 Tennoidai, Tsukuba, Ibaraki 305-8571, Japan

[‡]National Institute for Materials Science, Tsukuba, Ibaraki 305-0044, Japan

[§]Institute for Chemical Research, Kyoto University, Gokasho, Uji, Kyoto 611-0011, Japan

Supporting Information

ABSTRACT: Ion exchange of ionic semiconductor nanoparticles (NPs) is a facile method for the synthesis of type-II semiconductor heterostructured NPs with staggered alignment of band edges for photoelectric applications. Through consideration of the crystallographic orientation and strain at the heterointerface, well-designed heterostructures can be constructed through ion exchange reactions. Here we report the selective synthesis of anisotropically phase-segregated cadmium sulfide (CdS)/ cadmium telluride (CdTe) heterodimers via a novel anion exchange reaction of CdS NPs with an organic telluride precursor. The wurtzite-CdS/zinc blende-CdTe heterodimers in this study resulted from spontaneous phase segregation induced by the differences in the crystal structures of the two phases, accompanying a centrosymmetry breaking of the spherical CdS NPs. The CdS/CdTe heterodimers exhibited photoinduced spatial charge separation because of their staggered band-edge alignment.

Heterostructured NPs, in which two or more distinct inorganic materials are connected together,[1,2] are expected to provide new ways to manipulate wave functions,[3] plasmon resonances,[4] and spin.[5] In semiconductor heterostructures, the choice of semiconductor materials allows control of the manner of confinement of the electron and hole wave functions in NPs. Type-II heterostructured NPs with a staggered alignment of band edges at the heterointerface can promote spatial charge separation of the electron and hole in different parts of the heterostructure for photocatalytic and photovoltaic applications.[6]

Heterostructured NPs can be synthesized by partial transformation of NPs into heterostructures. Several studies have demonstrated that partial ion exchange reactions of ionic semiconductor NPs are effective for selective synthesis of semiconductor heterostructures.[7] Because smaller ionic crystals have a larger surface-to-volume ratio and enhanced reactivity, ionic NPs exhibit unusually high ion exchange rates relative to the bulk form. Cation exchange reactions in metal chalcogenide NPs have been studied extensively,[7a−d] although few examples of anion exchange reactions of ionic NPs have been reported.[7e] Increased understanding of anion exchange reactions will allow the range of structure control of ionic NPs to be extended. The choice of materials is also important for control of the morphologies of the resulting heterostructures because the strain between the already formed phases (seeds) and newly grown phases induces spontaneous phase segregation during the ion exchange reaction.[7b,c]

Here we report a novel anion exchange reaction of ionic CdS NPs with tri-*n*-octylphosphine telluride (TOP═Te) to form CdS/CdTe heterodimers. The CdS/CdTe combination was chosen because this heterointerface forms a type-II band-edge alignment.[8] The thermodynamically stable phases of CdS and CdTe crystals are wurtzite (*w*) and zinc blende (*zb*), respectively, and large strain at the heterointerface should induce spontaneous phase segregation. The anion exchange reaction proceeded smoothly to give anisotropically phase-segregated CdS/CdTe heterodimers with one heterointerface as an intermediate during formation of the completely exchanged product, CdTe NPs. Spontaneous formation of CdS/CdTe heterodimers took place because of the strain relaxation of the different crystallographic orientations of the *w*-CdS and *zb*-CdTe phases. Atomic-resolution high-angle annular dark-field (HAADF) scanning transmission electron microscopy (STEM) observations revealed that the heterointerface was *w*-CdS (0001)/*zb*-CdTe ($\overline{111}$). Transient absorption spectroscopy demonstrated that photoinduced one-directional charge separation occurred in CdS/CdTe heterodimers because of the type-II band-edge alignment with one heterointerface.

Anion exchange of the CdS NPs was performed as follows. Spherical *w*-CdS NPs (average diameter 10 nm; Figure 1a) were mixed with oleylamine under a nitrogen atmosphere at 260 °C. A TOP solution of Te powder was then swiftly injected into the mixture. The solution gradually changed color from yellow to dark-brown. Evolution of the products was monitored by X-ray fluorescence (XRF) spectroscopy (Figure 1f). The mole fraction of Cd was held at ∼50% throughout the reaction. The mole fractions of S and Te monotonically decreased and increased, respectively, indicating that the CdS NPs were successfully converted into CdTe NPs via an anion exchange reaction. Morphological changes in the NPs were monitored by TEM (Figure 1a−e). Earlier in the reaction (at 30 min), NPs with two spherical sections, one of which was a small CdTe head, were observed (Figure 1b).

Received: August 18, 2011
Published: October 06, 2011

dx.doi.org/10.1021/ja2078224 | *J. Am. Chem. Soc.* 2011, 133, 17598–17601

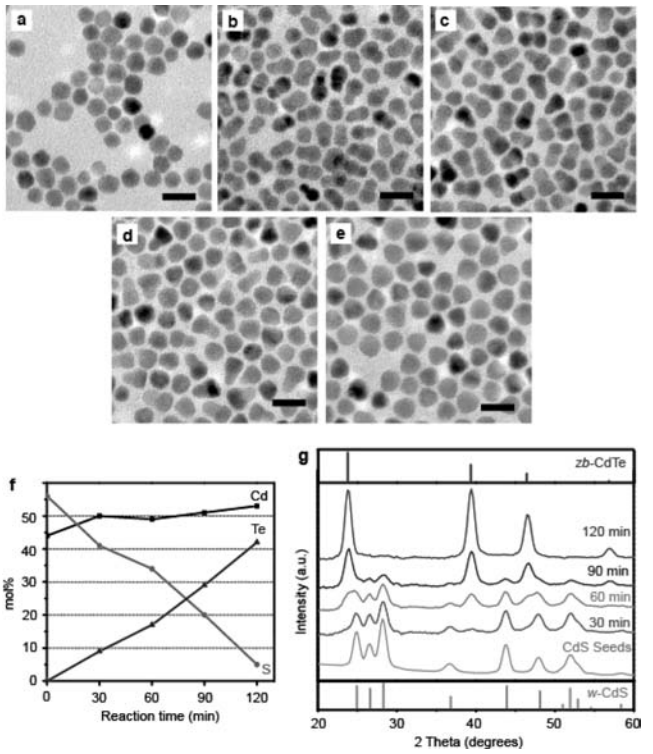

Figure 1. (a–e) TEM images of the products obtained by the anion exchange reaction of 10 nm *w*-CdS NPs with TOP═Te at 260 °C for (a) 0, (b) 30, (c) 60, (d) 90, and (e) 120 min. Scale bars = 20 nm. (f, g) Temporal changes in (f) the composition as estimated by XRF and (g) the crystal structure during the anion exchange reaction of 10 nm CdS NPs at 260 °C.

As the reaction progressed, the CdTe phases grew larger and the CdS phases shrank (Figure 1b–d). The CdS phases had almost completely disappeared at 120 min (Figure 1e). This phase conversion was also supported by the temporal change of the X-ray diffraction (XRD) patterns of the products (Figure 1g), in which the peaks assigned to the *w*-CdS phase decreased in intensity and those assigned to the *zb*-CdTe phase increased in intensity as the reaction progressed. The XRD patterns of the partially converted products formed at 30–90 min showed superimposed diffraction peaks for both the *w*-CdS and *zb*-CdTe phases, which indicates that the alloy ($CdS_{1-x}Te_x$) did not form throughout the reaction. At >120 min, almost complete transformation to *zb*-CdTe was observed in the XRD patterns, as in the TEM observations.

A HAADF-STEM image of partially anion-exchanged CdS/CdTe heterodimers clearly showed anisotropic phase segregation of the CdS and CdTe phases (Figure 2a). The brightness of the HAADF image is related to the mean atomic number, and the brighter and darker phases correspond to the CdTe and CdS phases, respectively. A high-resolution bright-field (BF) STEM image of the epitaxial interface of a single heterodimer (Figure 2b) was obtained; it had an orientation relationship of *w*-CdS {0002}//*zb*-CdTe {111} and *w*-CdS ⟨11$\bar{2}$0⟩//*zb*-CdTe ⟨110⟩. The CdS/CdTe heterodimers had only one heterojunction because of the lack of inversion symmetry along the *c* axis of the *w*-CdS.[9] The (0001) and (000$\bar{1}$) end facets of the *w*-CdS NPs are crystallographically nonequivalent because the (0001) and (000$\bar{1}$) planes are terminated by Cd^{2+} cations and S^{2-} anions, respectively. Consequently, the *w*-CdS

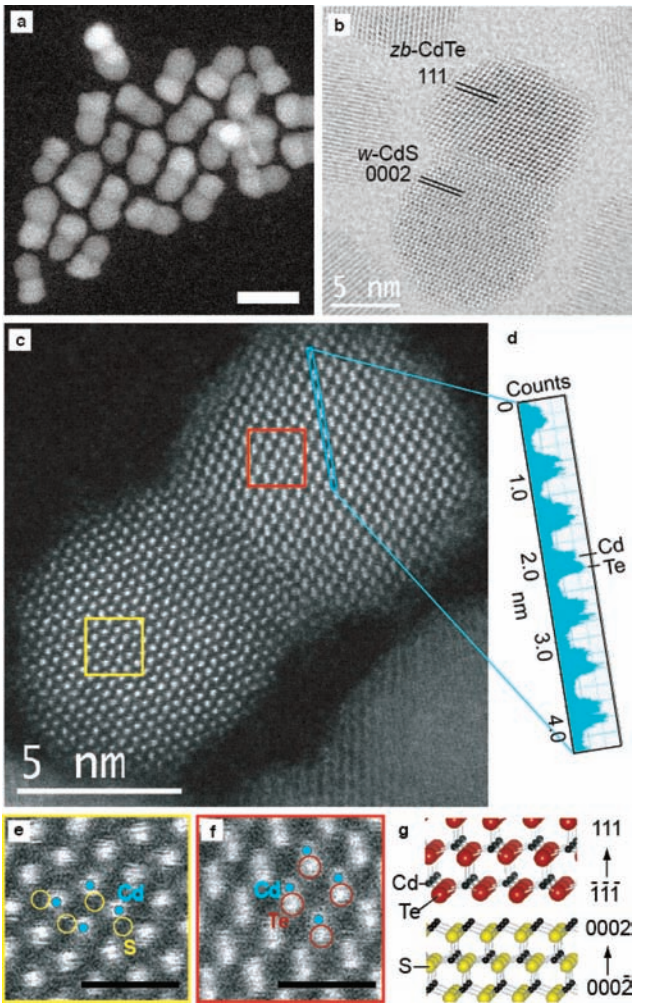

Figure 2. (a) HAADF-STEM and (b) BF-STEM images of CdS/CdTe heterodimers. (c) Atomic-resolution HAADF-STEM image of a single CdS/CdTe heterodimer. (d) *Z*-contrast profile of anion/cation pair columns in the blue rectangular region in (c). (e, f) Magnified images of the yellow and red rectangular regions for (e) *w*-CdS and (f) *zb*-CdTe phases in (c), respectively. Scale bars = 1 nm. (g) Illustration of the *w*-CdS/*zb*-CdTe heterointerface.

(0001) and (000$\bar{1}$) ends form different bonding arrangements at the *w*-CdS/*zb*-CdTe interface, at which *w*-CdS (0001)/*zb*-CdTe ($\bar{1}\bar{1}\bar{1}$) and *w*-CdS (000$\bar{1}$)/*zb*-CdTe (111) junctions are possibly formed by Cd–Te and Cd–S bonds, respectively. Atomic-resolution *Z*-contrast imaging with STEM (Figure 2c) was used to provide a better understanding of the interfacial structure of the *w*-CdS/*zb*-CdTe heterojunction.[10] Because atomic-number differences allow easy identification of cations and anions, the polar characteristics of the interface could be distinguished. Electron scattering by a column of Te ($Z = 52$) is stronger than that by a column of Cd ($Z = 48$), and thus, Te appears brighter than Cd in the *Z*-contrast image. The Cd^{2+}/Te^{2-} cation/anion pair columns could be distinguished from the *Z*-contrast profile (Figure 2d). For CdS, the S^{2-} anions ($Z = 16$) have darker *Z*-contrast than the Cd^{2+} cations. Thus, the Cd, Te, and S columns could be assigned as shown in Figure 2e,f. These observations revealed that the interface consisted of a Te-terminated ($\bar{1}\bar{1}\bar{1}$) plane of *zb*-CdTe and a Cd-terminated (0001) plane of *w*-CdS (Figure 2g). This indicates that the *w*-CdS (0001)/*zb*-CdTe ($\bar{1}\bar{1}\bar{1}$) interface is more stable than the *w*-CdS (000$\bar{1}$)/*zb*-CdTe (111)

dx.doi.org/10.1021/ja2078224 |*J. Am. Chem. Soc.* 2011, 133, 17598–17601

interface, which leads to the formation of only one CdS/CdTe heterojunction in a single heterodimer. The preferential formation of the *w*-CdS (0001)/*zb*-CdTe ($\overline{111}$) interface can be explained by the surface free energy of the CdTe phase. If *zb*-CdTe nucleates on the S-terminated *w*-CdS (000$\overline{1}$), *zb*-CdTe phases expose Te-terminated {$\overline{111}$} planes, on which passivation by polar ligands (e.g., oleylamine and TOP) is difficult because of the electrostatic repulsion.[3a] By contrast, when *zb*-CdTe nucleates on the Cd-terminated *w*-CdS (0001) plane, the *zb*-CdTe phases expose Cd-terminated {111} planes, on which the polar ligands can easily adsorb. Passivation of the NP surface by the protecting ligands greatly reduces the surface free energy of the *zb*-CdTe phases and makes them thermodynamically stable.

According to the detailed STEM observations, the brightness of the anion columns near the interface was between that of Te and S, which indicates that Te and S coexist along the zone axis, probably because the CdTe phase partially coats the spherical CdS phase, as mentioned below [Figure S1 in the Supporting Information (SI)]. The lattice spacing of this intermediate Z-contrast phase is ∼3% larger than that of *w*-CdS and ∼6% smaller than that of *zb*-CdTe, which suggests that alloying may also take place within the three layers near the interface to relax the lattice mismatch of ∼11% (Figure S1). However, alloying could not be identified by the XRD measurement because the volumes of the alloy phases were much smaller than those of the pure CdS and CdTe phases.

Generally, partial ion exchange of spherical NPs yields spherical core− or yolk−shell -type NPs with retained centrosymmetry.[7d,e] The centrosymmetry breaking of the spherical CdS NPs in this case might result from the large lattice mismatch between *w*-CdS and *zb*-CdTe (11%) and/or their crystal structure differences. Alivisatos and co-workers reported that bulk heteroepitaxy between *w*-ZnO and *w*-ZnS can proceed even though the lattice mismatch is large (∼18%),[7e] which suggests that the main reason for the *w*-CdS/*zb*-CdTe phase segregation in this study is the difference in their crystal structures. Previously reported core−shell NPs obtained by partial ion exchange of spherical NPs have the same symmetrical crystal structure (i.e., *w*-ZnO/*w*-ZnS[7e] and rock salt PbSe/*zb*-CdSe[7d] core−shell NPs). In CdE (E = S, Se, Te), one crystal layer is composed of a Cd and E pair as a single bilayer. Zinc blende and wurtzite sequences are typically ABCABC and ABABAB (each letter represents a bilayer), respectively, which implies that the deposition of *zb*-CdTe onto the planes parallel to the *c* axis of *w*-CdS ({10$\overline{1}$0} and {11$\overline{2}$0}) is strongly inhibited because the atomic positions do not conform symmetrically. The *zb*-CdTe phase was connected to the *w*-CdS {0002} facet, which is crystallographically equivalent to the {111} facet of the zinc blende lattice (threefold-symmetric configuration of cations and anions).

Next, the formation mechanism of the CdS/CdTe heterodimers was investigated by monitoring their growth process. To observe the structural evolution of CdS/CdTe heterodimers, large *w*-CdS NPs (19 nm) were used as the seed NPs. The detailed TEM observations suggest that the Volmer -Weber-type transformation[11] occurs in this anion exchange reaction (see SI and Figure S2 for detail).

To explore the reaction mechanism of the anion exchange reaction, some control experiments were carried out. The anion exchange reaction from CdTe to CdS was minimal at 260 °C after 120 min (Figure S3). When CdS NPs were heated at 260 °C for 120 min with TOP in the absence of Te, no significant change in size or composition was observed (Figure S4). These results

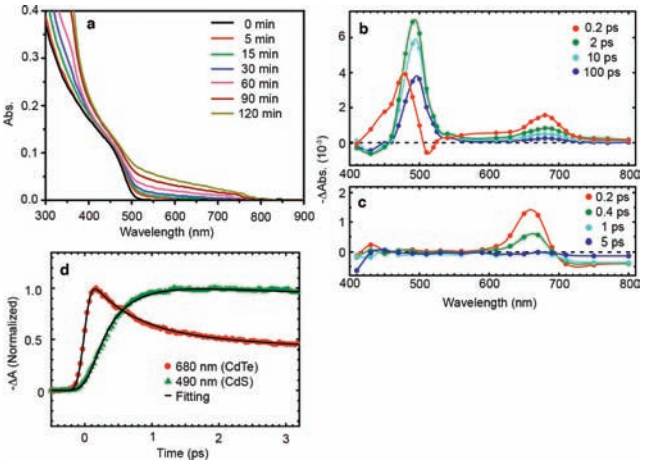

Figure 3. (a) Temporal evolution of UV−vis−NIR absorption spectra during the anion exchange reaction of *w*-CdS with TOP═Te. (b, c) Transient absorption spectra of (b) CdS/CdTe heterodimers and (c) a mixture of *w*-CdS and *zb*-CdTe NPs (λ_{pump} = 600 nm). (d) Kinetics of CdTe and CdS state-filling signals in (b) during the first 3 ps after photoexcitation.

strongly suggest that the driving force of the anion exchange reaction of the CdS NPs with TOP═Te is the favorable formation of the thermodynamically more stable TOP═S over TOP═Te because the binding energy of the P═S bond is higher than that of the P═Te bond [e.g., the binding energy for tri-*n*-butylphosphine sulfide (TBP═S) is 403 kJ/mol vs 218 kJ/mol for TBP═Te).[12] When the CdS NPs reacted with TOP═Se, the anion exchange was small (Figure S5), probably because the difference in the P═E binding energies of TOP═Se and TOP═S is not large enough to induce fast anion exchange from CdS to CdSe;[12] the P═Se binding energy in TBP═Se is 315 kJ/mol. When TOP═Te was replaced with TBP═Te, the anion exchange rate increased because the shorter alkyl chains of the tri-*n*-alkylphosphine increased the reactivity of the P atom by reducing the steric hindrance (Figure S6). This result also suggests that the conversion from P═Te to P═S plays a key role in the anion exchange reaction.

Finally, the structure-specific optical properties of the *w*-CdS/*zb*-CdTe heterodimers were investigated. Basically, an increase in the absorbance of the products in the near-IR region was accompanied by growth of the CdTe phase (band gap energy = 1.44 eV; Figure 3a). From the viewpoint of the structure-specific properties, type-II band-edge alignment between CdS and CdTe allows the realization of spatial carrier separation in a heterodimer, in which photoexcited electrons and holes are confined in the CdS and CdTe phases, respectively.[13] To understand the photoexcited carrier dynamics in the CdS/CdTe heterodimers, femtosecond transient absorption spectroscopy measurements were conducted (Figure 3b). The pump pulse was tuned to 600 nm to photoexcite only the CdTe phases. With a short delay between the pump and probe pulses (0.2 ps), an induced absorption ($\Delta A > 0$) at 510 nm and two bleaching signals ($\Delta A < 0$) at 475 and 680 nm were observed. Induced absorption (510 nm) below the steady-state exciton band of CdS (475 nm) would result from the red shift of the quantized levels of the heterodimers. This could occur from the Stark effect, which is derived from the photoexcited carrier-induced local fields in the heterodimers, or Coulomb multiparticle interactions in the

dx.doi.org/10.1021/ja2078224 |*J. Am. Chem. Soc.* 2011, 133, 17598–17601

heterodimers.[14] The two bleaching peaks at 490 and 680 nm observed with a >2 ps delay were associated with the CdS and CdTe exciton transitions by state filling, respectively. Because the 600 nm pump pulse only excites electrons in the CdTe phases, the state filling in CdS should be induced by electron injection from the CdTe phase to the CdS phase. Temporal changes of the transient absorption signals at the CdTe (680 nm) and CdS (490 nm) transitions within 3 ps after photoexcitation (Figure 3d) revealed an ultrafast decay of the CdTe bleaching, which was accompanied by a subsequent increase in the CdS bleaching. The relatively slow rise in the bleaching of the CdS band edge transition arises from the electron transfer from the conduction band of CdTe to that of CdS. Because of the transient absorption signals resulting from the red shift of the CdS transition at very short delay times (0.2 ps) as mentioned above, an electron transfer time of ~440 fs from the increase in CdS bleaching (Figure 3d) was evaluated (see the SI). This electron transfer time is approximately equal to the initial fast decay time of CdTe bleaching. From the ratio of the amplitude of the initial fast decay component to that of the slow decay component in the CdTe bleaching signal, the charge transfer efficiency from CdTe to CdS was estimated to be 50%. This estimation gives the minimum value of the transfer efficiency because the state-filling-induced bleaching signal also includes the signal from the holes remaining in the CdTe valence band. The spatial charge separation was further supported by considerable quenching of the CdS emission in the photoluminescence spectrum of the CdS/CdTe heterodimers. As a control, femtosecond transient spectra of a mixture of CdTe and CdS NPs were also measured (Figure S7). The transient absorption spectra of the mixed NPs exhibited bleaching of the CdTe band-edge transition but no bleaching of the CdS band-edge transition (Figure 3c), indicating that the photoexcited electrons in the conduction band of the CdTe phases are not transferred to the CdS phases. These results strongly demonstrate that the CdS/CdTe heterointerface effectively produces photoexcited spatial charge separation.

In conclusion, anisotropically phase-segregated CdS/CdTe heterodimers were spontaneously formed via the partial anion exchange reaction of CdS NPs with TOP═Te. The differences in the crystal structures of *w*-CdS and *zb*-CdTe played a key role in the spontaneous anisotropic phase segregation. The different polar characteristics of the *w*-CdS (0001) and (000$\bar{1}$) surfaces led to one-sided growth of the *zb*-CdTe phase. Favorable formation of the P═S bond, which is thermodynamically more stable than the P═Te bond, is responsible for this anion exchange reaction. The CdS/CdTe heterodimers exhibited spatial charge separation at the heterointerface, and this could be applied to photovoltaic and photocatalytic applications. Furthermore, only one type-II heterointerface can achieve one-directional charge transfer, which is a significant advantage in photovoltaic applications.

■ ASSOCIATED CONTENT

Ⓢ Supporting Information. Experimental and analytical protocols, additional TEM images, XRD patterns, temporal compositional evolutions, and absorption spectra. This material is available free of charge via the Internet at http://pubs.acs.org.

■ AUTHOR INFORMATION

Corresponding Author
teranisi@scl.kyoto-u.ac.jp

■ ACKNOWLEDGMENT

We thank Dr. A. Furube (National Institute of Advanced Industrial Science and Technology, Tsukuba, Japan) for his advice. This work was supported by KAKENHI (23245028 to T.T.) from JSPS and a JSPS Research Fellowship for Young Scientists (20429 to M.S. and 22-55312 to S.T.) and partially supported by KAKENHI (21340084 to Y.K.) from JSPS and the Nanotechnology Network of MEXT.

■ REFERENCES

(1) (a) Cozzoli, P. D.; Pellegrino, T.; Manna, L. *Chem. Soc. Rev.* **2006**, *35*, 1195. (b) Casavola, M.; Buonsanti, R.; Caputo, G.; Cozzoli, P. D. *Eur. J. Inorg. Chem.* **2008**, 837. (c) Carbone, L.; Cozzoli, P. D. *Nano Today* **2010**, *5*, 449.

(2) (a) Teranishi, T.; Inoue, Y.; Nakaya, M.; Oumi, Y.; Sano, T. *J. Am. Chem. Soc.* **2004**, *126*, 9915. (b) Teranishi, T.; Saruyama, M.; Nakaya, M.; Kanehara, M. *Angew. Chem., Int. Ed.* **2007**, *46*, 1713. (c) Teranishi, T.; Wachi, A.; Kanehara, M.; Shoji, T.; Sakuma, N.; Nakaya, M. *J. Am. Chem. Soc.* **2008**, *130*, 4210. (d) Teranishi, T.; Saruyama, M.; Kanehara, M. *Nanoscale* **2009**, *1*, 225.

(3) (a) Smith, A. M.; Nie, S. *Acc. Chem. Res.* **2010**, *43*, 190. (b) de Mello Donegá, C. *Chem. Soc. Rev.* **2011**, *40*, 1512.

(4) Bardhan, R.; Grady, N. K.; Ali, T.; Halas, N. J. *ACS Nano* **2010**, *4*, 6169.

(5) Zhang, J.; Tang, Y.; Lee, K.; Ouyang, M. *Nature* **2010**, *466*, 91.

(6) (a) Kumar, S.; Jones, M.; Lo, S. S.; Scholes, G. D. *Small* **2007**, *3*, 1633. (b) Hewa-Kasakarage, N. N.; Kirsanova, M.; Nemchinov, A.; Schmall, N.; El-Khoury, P. Z.; Tarnovsky, A. N.; Zamkov, M. *J. Am. Chem. Soc.* **2009**, *131*, 1328. (c) Regulacio, M. D.; Ye, C.; Lim, S. H.; Bosman, M.; Polavarapu, L.; Koh, W. L.; Zhang, J.; Xu, Q.-H.; Han, M.-Y. *J. Am. Chem. Soc.* **2011**, *133*, 2052. (d) Nonoguchi, Y.; Nakashima, T.; Kawai, T. *Small* **2009**, *5*, 2403.

(7) (a) Son, D. H.; Hughes, S. M.; Yin, Y.; Alivisatos, A. P. *Science* **2004**, *306*, 1009. (b) Robinson, R. D.; Sadtler, B.; Demchenko, D. O.; Erdonmez, C. K.; Wang, L.; Alivisatos, A. P. *Science* **2007**, *317*, 355. (c) Sadtler, B.; Demchenko, D. O.; Zheng, H.; Hughes, S. M.; Merkle, M. G.; Dahmen, U.; Wang, L.; Alivisatos, A. P. *J. Am. Chem. Soc.* **2009**, *131*, 5285. (d) Pietryga, J. M.; Werder, D. J.; Williams, D. J.; Casson, J. L.; Schaller, R. D.; Klimov, V. I.; Hollingsworth, J. A. *J. Am. Chem. Soc.* **2008**, *130*, 4879. (e) Park, J.; Zheng, H.; Jun, Y.; Alivisatos, A. P. *J. Am. Chem. Soc.* **2009**, *131*, 13943.

(8) Romeo, A.; Terheggen, M.; Abou-Ras, D.; Bätzner, D. L.; Haug, F.-J.; Kälin, M.; Rudmann, D.; Tiwari, A. N. *Prog. Photovoltaics* **2004**, *12*, 93.

(9) Peng, Z. A.; Peng, X. *J. Am. Chem. Soc.* **2001**, *123*, 1389.

(10) (a) McDaniel, H.; Zuo, J. M.; Shim, M. *J. Am. Chem. Soc.* **2010**, *132*, 3286. (b) McBride, J. R.; Kippeny, T. C.; Pennycook, S. J.; Rosenthal, S. J. *Nano Lett.* **2004**, *4*, 1279. (c) Palking, M. J.; Urban, J. J.; Milliron, D. J.; Zheng, H.; Chan, E.; Caldwell, M. A.; Raoux, S.; Kisielowski, C. F.; Ager, J. W., III; Ramesh, R.; Alivisatos, A. P. *Nano Lett.* **2011**, *11*, 1147.

(11) (a) Gu, H.; Zheng, R.; Zhang, X.; Xu, B. *J. Am. Chem. Soc.* **2004**, *126*, 5664. (b) Kwon, K. W.; Shim, M. *J. Am. Chem. Soc.* **2005**, *127*, 10269.

(12) Capps, K. B.; Wixmerten, B.; Bauer, A.; Hoff, C. D. *Inorg. Chem.* **1998**, *37*, 2861.

(13) (a) Schöps, O.; Le Thomas, N.; Woggon, U.; Artemyev, M. V. *J. Phys. Chem. B* **2006**, *110*, 2074. (b) Zeng, Q.; Kong, X.; Sun, Y.; Zhang, Y.; Tu, L.; Zhao, J.; Zhang, H. *J. Phys. Chem. C* **2008**, *112*, 8587. (c) Deng, Z.; Schulz, O.; Lin, S.; Ding, B.; Liu, X.; Wei, X.; Ros, R.; Yan, H.; Liu, Y. *J. Am. Chem. Soc.* **2010**, *132*, 5592. (d) Dorfs, D.; Franzl, T.; Osovsky, R.; Brumer, M.; Lifshitz, F.; Klar, T. A.; Eychmüller, A. *Small* **2008**, *4*, 1148.

(14) (a) Norris, D. J.; Sacra, A.; Murray, C. B.; Bawendi, M. G. *Phys. Rev. Lett.* **1994**, *72*, 2612. (b) Klimov, V.; Hunsche, S.; Kurz, H. *Phys. Rev. B* **1994**, *50*, 8110.